The Electrophysiological Markers of Statistically Learned Attentional Enhancement: Evidence for a Saliency-based Mechanism

Dock H. Duncan[1,2], Jan Theeuwes[1,2,3], and Dirk van Moorselaar[1,2]

Abstract

■ It is well established that attention can be sharpened through the process of statistical learning (e.g., visual search becomes faster when targets appear at high-relative-to-low probability locations). Although this process of statistically learned attentional enhancement differs behaviorally from the well-studied top–down and bottom–up forms of attention, relatively little work has been done to characterize the electrophysiological correlates of statistically learned attentional enhancement. It thus remains unclear whether statistically learned enhancement recruits any of the same cognitive mechanisms as top–down or bottom–up attention. In the current study, EEG data were collected while participants searched for an ambiguous unique shape in a visual array (the additional singleton task). Unbeknownst to the participants, targets appeared more frequently in one location in space (probability cuing). Encephalographic data were then analyzed in two phases: an anticipatory phase and a reactive phase. In the anticipatory phase preceding search stimuli onset, alpha lateralization as well as the Anterior Directing Attention Negativity and Late Directing Attention Positivity components—signs of preparatory attention known to characterize top–down enhancement—were tested. In the reactive phase, the N2pc component—a well-studied marker of target processing—was examined following stimuli onset. Our results showed that statistically learned attentional enhancement is not characterized by any of the well-known anticipatory markers of top–down attention; yet targets at high probability locations did reliably evoke larger N2pc amplitudes, a finding that is associated with bottom–up attention and saliency. Overall, our findings are consistent with the notion that statistically learned attentional enhancement increases the perceptual salience of items appearing at high-probability locations relative to low-probability locations. ■

INTRODUCTION

When we look upon a scene, several factors coalesce to determine how attention is deployed—these include the low-level feature contrasts within a scene (a red stop sign automatically pops out from a gray background) and our current search priorities (we notice street names when trying to find a specific address). Traditionally, attentional selection was assumed to be solely determined by the interaction between these bottom–up (salience-driven) and top–down (goal-directed) factors (Theeuwes, 2010; Egeth & Yantis, 1997; Wolfe, 1994; Koch & Ullman, 1984). However, it is now clear that attentional deployment is also affected by our past experiences with selecting stimuli (Theeuwes, 2019; Jiang, 2018; Awh, Belopolsky, & Theeuwes, 2012; Geng & Behrmann, 2005). The influence of past experiences on future attentional behavior is known as selection history, a category of phenomena including intertrial priming, reward learning, and statistical learning (Anderson et al., 2021; Failing & Theeuwes, 2018).

There is a general consensus that when targets appear more often in one location than in other locations, participants implicitly learn this statistical distribution and subsequently detect targets faster at high than at low probability locations (Geng & Behrmann, 2002, 2005). This attentional effect has been shown to scale monotonically with the probability that targets appear in one particular spatial location (Zhang, Yang, Wang, & Theeuwes, 2022), demonstrating that participants can optimally mold their attentional biases to match the statistical regularities of the task at hand in a process known as statistical learning (see Theeuwes, Bogaerts, & van Moorselaar, 2022).

While top–down and bottom–up influences on attentional selection have been intensively studied both at a behavioral (Luck, Gaspelin, Folk, Remington, & Theeuwes, 2021) and neural level (Fecteau & Munoz, 2006; Desimone & Duncan, 1995), surprisingly little neuroimaging work has investigated the cognitive mechanisms underlying statistically learned attentional enhancement. The current EEG study remedies this by describing the encephalographic characteristics of statistically learned attentional enhancement with special focus on its overlap with known markers of top–down and bottom–up attention. We focused on two search phases: the anticipatory phase before display onset

[1]Vrije Universiteit Amsterdam, The Netherlands, [2]Institute Brain and Behavior Amsterdam (iBBA), The Netherlands, [3]ISPA-Instituto Universitario, Lisbon, Portugal

Journal of Cognitive Neuroscience 35:12, pp. 2110–2125
https://doi.org/10.1162/jocn_a_02066

and the reactive phase following display onset. In our anticipatory analysis, we investigated well-studied preparatory indexes of top–down attention. Specifically, during the intertrial period, we examined alpha lateralization, a marker of attentional orienting (Rihs, Michel, & Thut, 2007; Worden, Foxe, Wang, & Simpson, 2000), as well as the Anterior Directing Attention Negativity (ADAN) and Late Directing Attention Positivity (LDAP) components, two well-studied components of top–down attentional preparation (Eimer, van Velzen, & Driver, 2002; Nobre, Sebestyen, & Miniussi, 2000; Harter, Miller, Price, LaLonde, & Keyes, 1989), to see if these components were shared between top–down and statistically learned forms of attentional enhancement. In the reactive analysis, we focused on the N2pc, a known marker of target processing (Eimer, 1996).

Broadly, we expected that if statistically learned attentional enhancement was mediated by the same mechanisms as top–down attention, then we should see robust anticipatory effects in the alpha band as well as in the ADAN and LDAP components. Furthermore, we would expect the N2pc either to be insensitive to the high-probability (HP) location (Kiss, Van Velzen, & Eimer, 2008) or to change only in its latency, with expected stimuli being processed faster than stimuli at rare locations (Foster, Bsales, & Awh, 2020). On the other hand, recent theories have proposed that selection history effects are mediated by quite distinct mechanisms from top–down attention; the recently proposed synaptic account of statistical learning specifically posits that statistically learned enhancement and suppression are mediated by changes in the latent excitability of spatially tuned neurons' (i.e., the putative spatial priority map) increase attentional priority at HP locations in an activity silent manner (Duncan, van Moorselaar, & Theeuwes, 2023; Ferrante, Zhigalov, Hickey, & Jensen, 2023; van Moorselaar, Lampers, Cordesius, & Slagter, 2020). Under this theory, we would expect none of the well-known markers of anticipatory top–down attention, but differences in N2pc activity would remain possible. Specifically, if statistically learned attentional enhancement results in greater perceptual salience of items at expected locations, a result of the increased neural excitability of items in this region of space, then an increased N2pc amplitude would be expected as has previously been shown when modifying a targets relative saliency from its background (Töllner, Zehetleitner, Gramann, & Müller, 2011; Mazza, Turatto, & Caramazza, 2009).

To briefly preview our results, our findings are in line with the synaptic account of statistical learning, providing novel insights into the distinct mechanisms underlying statistical learning attentional enhancement. Furthermore, in addition to providing an encephalographic characterization of a well-studied behavioral effect, our results also provide evidence that the behavioral benefits of probability cuing stem from an increase in perceptual salience at HP target locations.

METHODS

Participants

This article reports novel analyses of data previously presented in Duncan and colleagues (2023). The sample size of 24 participants was thus selected based on the expected effect size from that project; however, this sample size also exceeds that of what is typically used in other ERP and time–frequency studies (Foster et al., 2020; Wang, van Driel, Ort, & Theeuwes, 2019). Out of the original sample, two participants were excluded during reanalysis because their eye tracking data revealed that they deviated from fixation on more than 30% of trials (see eye tracking methods below—note this was not an issue for published results as they focused on a different window of interest). The final data set of analysis thus consisted of 22 participants (17 women, average age 21 years). The study was conducted in the Brain and Behavior labs at Vrije Universiteit Amsterdam; all participants indicated normal or corrected-to-normal vision and reported no history of cognitive impairments. All participants additionally provided written informed consent before participation and were compensated with 25 € or equivalent course credit. The study conformed to the Declaration of Helsinki and was approved by the ethical review committee of the faculty.

Apparatus and Stimuli

Participants were seated in a sound-attenuated room with dim lighting 60 cm away from a 23.8 in., 1920 × 1080 pixel ASUS ROG STRIX XG248 LED monitor with a 240-Hz refresh rate, which displayed all stimuli. The behavioral task was programmed using OpenSesame (Mathôt, Schreij, & Theeuwes, 2012) and incorporated functions from the PsychoPy library of psychophysical tools (Peirce, 2007). EEG data were recorded using a 64-electrode cap with electrodes placed according to the International 10–10 system (Biosemi ActiveTwo system; biosemi.com), with two earlobe electrodes used as offline reference, and default Biosemi settings at a sampling rate of 512 Hz. External electrodes placed ~2 cm above and below the right eye, and ~1 cm lateral to the left and right lateral canthus were used to record VEOG and HEOG. Eye-tracking data were collected using an Eyelink 1000 (SR research) eye tracker that tracked both eyes. To maintain stability, participants used a headrest positioned 60 cm from the screen. Eye sampling varied between participants at 500, 1000, and 2000 Hz because of the different EEG laboratories used having different versions of the Eyelink 1000 with varying sampling limits. All participant data were later aligned with the EEG data during preprocessing. Calibration occurred before the first block and at the halfway point for all participants. Additional calibrations were performed for some participants because of subtle changes in resting position in the chinrest or if noticeable drift in the eye signal was suspected by the experimenter.

All stimuli were presented on a black background. The fixation point (~1.1°) was that shown by Thaler, Schütz, Goodale, and Gegenfurtner (2013), to enforce stable fixation. The search display consisted of eight equally spaced shapes presented on an imaginary circle centered at fixation (radius = ~4.8°). Shapes could either be diamonds (82 × 82 px or ~2.1° × 2.1° square rotated 45°) or circles (diameter 90 px, ~2.4°) and could be colored either red (red, green, blue [RGB] 255,0,1) or green (RGB 0,128,0). All shapes also contained a horizontally or vertically oriented white line (70 px; ~1.8°, RGB 255,255,255). The displays were rendered such that each display contained one unique shape (i.e., the target), and on a subset of trials, one of the homogeneous shapes had a unique color (i.e., singleton distractor).

Procedure and Design

The task was a combination of the additional singleton task (Theeuwes, 1992) and the probability cuing task (Geng & Behrmann, 2005) where targets were presented more frequently in certain regions in space (HP locations; see Figure 1A for an example of a task display). This sort of task has been shown to lead to an attentional facilitation at the HP location relative to the other low-probability locations (Huang, Donk, & Theeuwes, 2022; Gao & Theeuwes, 2020; Ferrante et al., 2018; Geng & Behrmann, 2005). Trials began with a fixation point onset, which lasted between 1.3 and 1.7 sec. On 50% of trials, a high contrast, task-irrelevant ping was presented for 200 msec sometime between 700 and 900 msec after fixation onset (see Duncan et al., 2023, or a neural analysis centered on these perturbations). These trials were first analyzed separately from trials in which the screen remained blank for the entire intertrial interval in our analysis of intertrial alpha. After that, the search display appeared and participants were instructed to find the unique shape singleton target and indicate the orientation of the line within by pressing either the "left" direction key (for "horizontal") or the "up" direction key (for "vertical"). The search arrays remained on screen for 2.5 sec or until participants provided a response. On a subset of trials (70%), the search display also contained a singleton distractor, which had to be ignored.

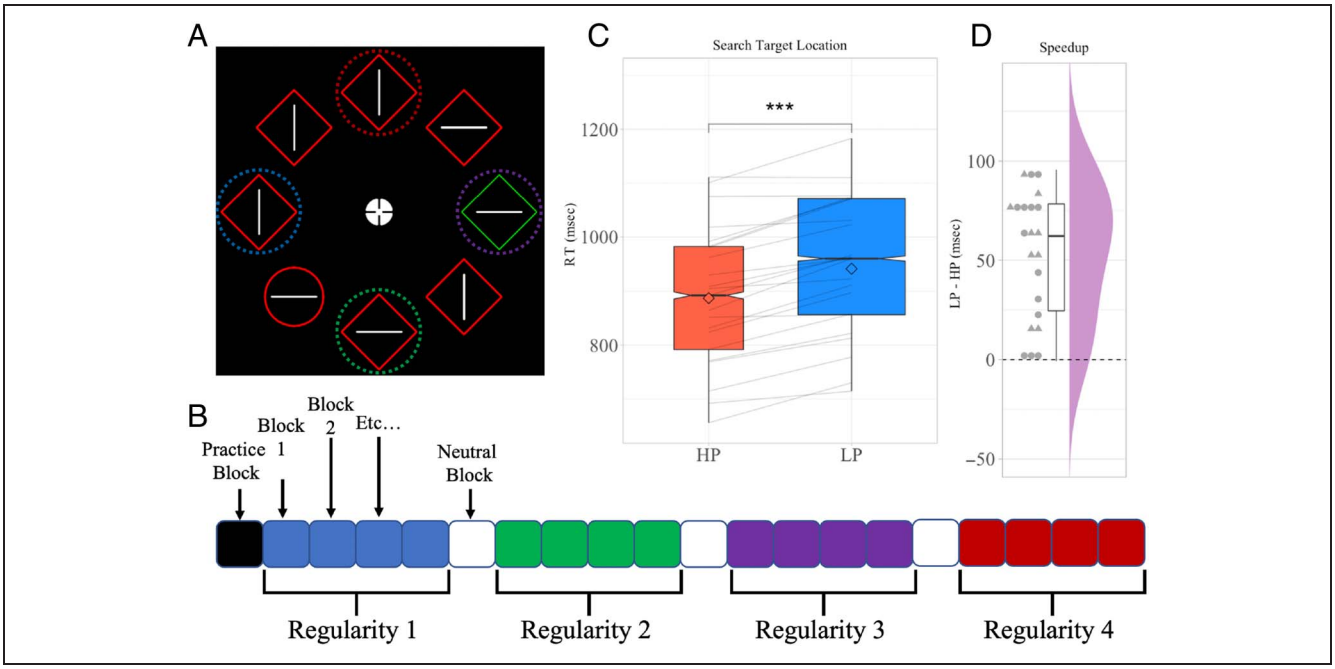

Figure 1. (A) An example of the additional singleton search display. In this task, participants look for a unique shape and report the orientation of the line held within this shape singleton. Although they perform this task, a color singleton is occasionally presented as a distractor. In the current study, an imbalance in the target location distribution evoked a probability cuing effect, where participants were implicitly trained to expect targets to appear in certain locations in space—as reflected by faster RTs. Denoted by the dotted circles are the four possible HP locations in space. Note that in the actual experiment, the four dotted circles did not appear. The colors of these circles correspond to the hypothetical block order shown in B Visual representation of the experiment's block structure. During the experiment, the HP target location occasionally shifted such that each participant would encounter a series of blocks where each of the four possible HP locations was active. These locations were the four cardinal locations (top, bottom, left, and right). High-probability locations would be stable for four blocks at a time before switching (symbolized by the four squares of the same color). Note that the four HP locations were counterbalanced between the participants such that no two participants encountered the four locations in the same order (the four locations shown in A are merely an example of one possible presentation order). In between HP blocks, three neutral blocks (represented by the white squares) were inserted. These blocks were meant to aid in the extinction of the previous probability cuing effect. (C) RTs when targets were presented in HP (red) trials or LP (blue) trials. Participants were reliably faster on HP trials than LP trials. (D) The individual speedup effect for each participant—calculated by taking each participants average RT on LP trials and subtracting their average RT for HP trials. Triangles represent participant averages for participants that indicated some awareness of the target regularity. Circles are participant averages for participants that reported no awareness of the target regularity.

Critically, targets did not appear at random locations across trials, but instead followed an undisclosed distributional regularity where they were disproportionately more likely to appear in one location than any other (37.5% of trials had targets at these locations). These HP target locations could either be the left, right, top, or bottom most positions in the search array. Furthermore, these locations shifted periodically (i.e., HP locations were used for four consecutive blocks before switching) during the experiment such that one location was only the high probability location for a certain amount of time in each experiment session (see Figure 1B; order counterbalanced across participants[1]). Thus, counter to typical probability cuing studies, condition averages reflected data across multiple display locations, rather than a single location benefit. Neutral blocks, in which targets appeared equally frequently at all eight locations, were inserted in between switches to give participants an opportunity to unlearn the previous HP location (Valsecchi & Turatto, 2021; Britton & Anderson, 2020; Duncan & Theeuwes, 2020) before moving on to a new HP condition.

The experiment itself consisted of 19 blocks of 56 trials each, plus one full practice block. In between blocks, participants received feedback on their performance (i.e., mean RT and accuracy) and were encouraged to take a short break. Upon completing the experiment, participants were asked whether they noticed any regularity to the target presentation. They were next asked to indicate where they believed the target was most likely to appear in the final block of the experiment, and finally they were asked if there were any other locations that they believed held the target more frequently at any time in the experiment.

EEG Preprocessing

After rereferencing all EEG data to the average of the two earlobe electrodes, a Hamming windowed finite impulse response filter was used to high-pass filter the data at 0.1 Hz to remove slow signal drifts. The continuous EEG signal was then segmented into epochs from 1500 msec before search onset to 1000 msec after search display onset. A different time window of −1000 msec to 500 msec was used to reject trials. Malfunctioning electrodes marked as bad by the experimenter during recording were temporarily removed before subsequent trial rejection and artifact correction. To identify EMG-contaminated epochs, an adapted version of an automated trial-rejection procedure was used, as implemented in Fieldtrip (Oostenveld, Fries, Maris, & Schoffelen, 2011). Muscle activity was specifically captured using a 110- to 140-Hz band-pass filter, and variable z-score thresholds per subject were allowed based on within-subject variance of z scores (de Vries, van Driel, & Olivers, 2017). Rather than immediately removing epochs exceeding the z-score threshold, the five electrodes that contributed most to accumulated z score within the time period containing the marked EMG artifact were first identified. An iterative procedure was then used to interpolate the five worst electrodes per marked epoch using spherical splines (Perrin, Pernier, Bertrand, & Echallier, 1989), checking whether that epoch still exceeded the determined z-score threshold after interpolation. Epochs were only dropped when after interpolation of the five worst electrodes the z-score threshold was still exceeded (~6% of trials rejected in this way per participant). Independent component analysis was then applied to the epoched data that had been high-pass filtered at 1 Hz using the "picard" method as implemented in MNE, to remove eye-blink components from the cleaned data (one component removed per participant). Finally, identified malfunctioning electrodes were interpolated using spherical splines.

Eye-tracking Exclusions

During the experiment, participants were instructed to keep their eyes locked on fixation at all times. To ensure this was the case, eye tracking data were recorded, with real time feedback given to participants when their eyes deviated from fixation in the form of a high-pitched beep. This eye tracking data were further used offline to exclude trials in which an eye movement was made. Using custom scripts, x, y positions were linearly interpolated in between the start and end of an eyeblink (± 20 msec). Trials with a fixation deviation > 1° of visual angle in a segment of continuous data of at least 40 msec in specific time windows (−1000 to 0 msec and −200 to 350 msec for the time–frequency and ERP analysis, respectively). In case a trial had missing eye tracker data, the HEOG recorded signal was examined instead for sudden jumps in the recorded signal—a known marker of saccades. A step method was used, with a window of 200 msec, a threshold of 15 μV, and a step size of 10 msec. In total, ~7% of trials in the ERP analysis and ~8% of trials in the alpha analysis were excluded because of eye movements (and as noted above, two participants from the original sample were excluded as more than 30% of trials were marked for exclusion).

Behavioral Analysis

Because only the left and right HP conditions were considered in our EEG analyses (and because the combined behavioral analysis with all HP locations has previously been reported; Duncan et al., 2023), our behavioral analysis was limited to these left- and right-sided HP blocks to ensure that the same behavioral enhancement was present in this limited data set as in the previously reported combined data set. Trials were excluded for analysis if the participant provided an incorrect response or if RT on that trial was more than 2.5 *SD*s away from the participant mean RT. For a more in-depth analysis of the behavioral data including an analysis of distractor conditions,

neutral block analyses, and the main target analysis including all blocks, then see Duncan and colleagues (2023).

Linear Mixed-model Analysis

To test the influence of intertrial priming, a logistic mixed-effects analysis was conducted (Bates, Mächler, Bolker, & Walker, 2015). Unlike the other statistical testing done on the behavioral data, our model was not restricted to data from blocks where the HP target location was on the left or right, but instead included all four HP locations. RTs were designated as the dependent variable with six fixed effects included. These effects were target condition (target at high or low probability location) as well as trial repetitions up to five trials[2] in the past (repetition yes/no). The random effects structure included a by-subject random intercept and random slopes for all fixed effects. The factors were coded as HP RT minus low probability RT, and for each repetition condition, they were coded as nonrepeat minus repeat. The model formula was as follows:

$$\begin{aligned} model = lmer\big(&RT \sim target_{high/low} + rept_1 + rept_2 + rept_3 \\ &+ rept_4 + rept_5 + \big(target_{high/low} + rept_1 + rept_2 \\ &+ rept_3 + rept_4 + rept_5 | subject_{id}\big)\big) \end{aligned}$$

In addition, restricted maximum likelihood was turned off and bobyqa optimization was used. The model had 17,345 observations and a loglikelihood of −121,796.7.

Temporal Frequency Analysis

For our temporal frequency analysis, separate analyses were conducted on trials in which a salient white ping was presented in the intertrial period, as well as on trials in which the screen remained static (trials were 50/50 across these conditions, see procedure and design). Following these separate analyses, all trials were collapsed into a single analysis and the results of all three analyses are reported separately (ping-only, no-ping, and combined). Our analyses were further restricted only to blocks in which the HP target was on the horizontal midline (left or right) as alpha lateralization has most commonly been studied in the context of horizontal cues (Klimesch, 2012).

Frequency-specific activity in the EEG signal was isolated using Morlet wavelet convolution to decompose the combined EEG signal into 25 logarithmically spaced steps of a frequency range from 4 to 40 Hz. To create complex Morlet wavelets, for each frequency, a sine wave ($e^{i2\pi ft}$, where i is the complex operator, f is frequency, and t is time) was multiplied by a Gaussian ($e^{-t\hat{}2/2s\hat{}2}$, where s is the width of the Gaussian). To keep a good trade-off between temporal and frequency precision, the Gaussian width was set as

$$s = \frac{\delta}{2\pi \mathbf{f}}$$

where ð represents the number of wavelet cycles, in 25 logarithmically spaced steps between 3 and 12. Frequency-domain convolution was then applied by multiplying the fast Fourier transform of the EEG data and Morlet wavelets. The resulting signal was converted back to the time domain using the inverse fast Fourier transform. Time-specific frequency power, which was down sampled by a factor of 4, was defined as the squared magnitude of the complex signal resulting from the convolution.

To investigate whether the presence of an HP location on the left or right of the horizontal midline resulted in a lateralization of alpha-power, we first calculated a lateralization index over the broadband frequency range; this was done by taking frequency-band data for all frequency bins calculated over contralateral sensors across all time points and subtracting them from those calculated over ipsilateral sensors. This matrix was then divided by the value of adding both ipsilateral and contralateral frequency values together (van Moorselaar et al., 2020):

$$\frac{contralateral - ipsilateral}{contralateral + ipsilateral}$$

A positive number then would indicate that contralateral power is larger than ipsilateral power, and vice versa for negative numbers. Critically, this index does not require a baseline. Statistical analyses were limited to electrode pairs PO7/8, PO3/4, and O1/2, which were selected on the basis of visual inspection of the topographic distribution of averaged alpha power (8–12 Hz; see Figure 2C) across the anticipatory time window (−1000 to 0 msec) and also were matched to those used in Wang and colleagues (2019) who previously found alpha lateralization following statistical distractor learning. This analysis was further repeated using only the average alpha band frequencies in both the total alpha band (8–12 Hz) as well as separately for upper- and lower-alpha bands (10–13 Hz and 7–10 Hz, respectively). For the alpha-specific analysis, the EEG signal was decomposed into six linearly spaced steps of a frequency range from 7 to 13 Hz.

In addition to the time–frequency analyses, a further Bayesian test of average alpha was done by taking the mean alpha lateralization value per participant in the anticipatory window. These values were then subject to a Bayesian one-sample t test using the default settings of the statistical analysis program JASP (Wagenmakers et al., 2018) and tested for evidence for the null (BF_{10}).

ERP Analysis

Three well-known ERP components were examined, split into two trial phases—an anticipatory phase focused only on the intertrial window and a reactive phase following search onset. In the anticipatory phase (−1000 to 0 msec relative to fixation onset), we examined the ADAN and LDAP components, two well-known indices of top–down

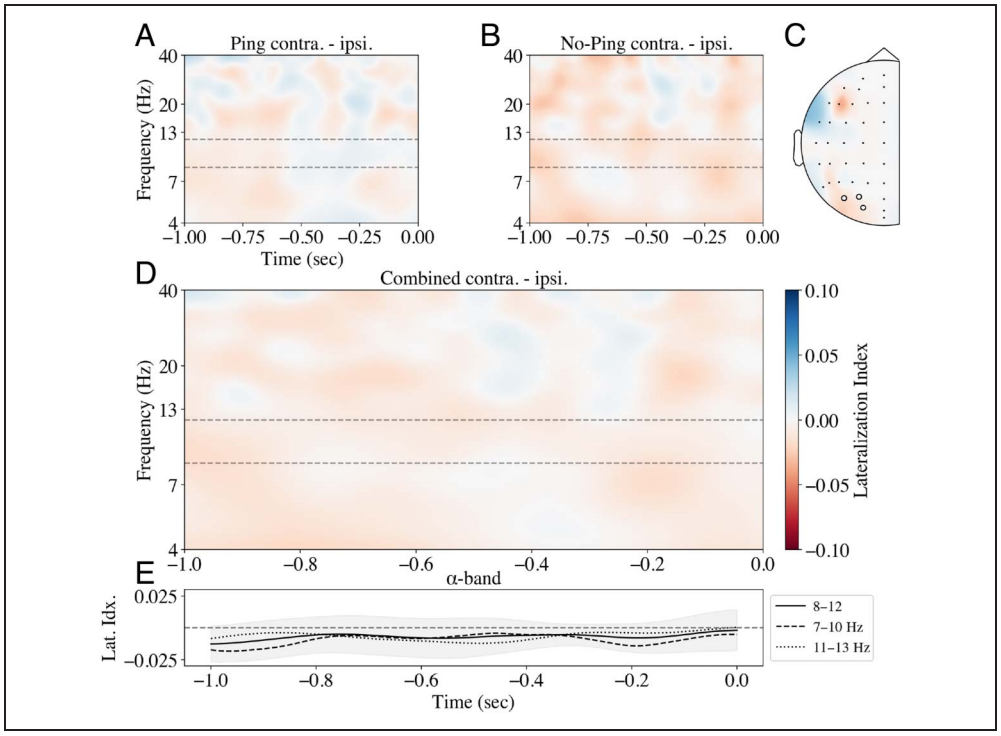

Figure 2. Broadband and alpha power lateralization in the intertrial period from posterior electrodes of interest. Lateralization scores for (A) ping and (B) no-ping trials. Lateralization was calculated by subtracting contralateral power from ipsilateral and dividing the result by their combined power. A cluster-based permutation analysis was conducted on these values to identify contiguous regions of significantly positive/negative values. No such clusters were found in either ping nor no-ping trials. Black dotted lines outline region between 7 and 10 Hz used in the main alpha analysis. Difference topography (C) and lateralized power difference across time (D) between contralateral and ipsilateral electrodes when combining ping and no-ping trials. (E) Averaged alpha difference for total alpha (solid line), lower alpha (dashed line), and upper alpha (dotted line). Light gray shaded represents 95% confidence interval of mean around total alpha condition. A cluster permutation test of each of these conditions (Figures 2A, B, D, and E) revealed no significant clusters deviated from zero (see Methods section).

attentional preparation (Eimer et al., 2002; Nobre et al., 2000; Harter et al., 1989). The ADAN and LDAP components are often examined following the onset of an informative cue. However, because our experiment did not use a cue, ERPs were instead yoked to the neutral fixation onset. Electrode selection for our ADAN and LDAP analysis were informed by previous research (Myers, Walther, Wallis, Stokes, & Nobre, 2015; Murray, Nobre, & Stokes, 2011). Specifically, the ADAN component included C3/4 and FC3/4, whereas the LDAP included the PO7/8 and O1/2 sensors.

For our analysis of the reactive phase following stimuli onset (−200 to 600 msec), we examined the target evoked N2pc component, a well-known marker of target processing (Mazza et al., 2009; Eimer, 1996; Luck & Hillyard, 1994). The PO7/8, PO3/4, and O1/2 sensors were selected for our N2pc analysis; these electrodes are commonly used to study the N2pc (Luck, 2014) and also showed the largest effect upon visual inspection of the condition averaged waveform. In addition, rather than selecting our N2pc window based on previous work, we instead centered it on the peak of the condition averaged difference wave, which has the advantage that condition differences do not bias the selected window, and hence, the selected window provides a fair comparison between conditions. The N2pc window was further split into an early and late phase, as has been done previously (Eimer, Kiss, & Cheung, 2010; Holmes, Bradley, Nielsen, & Mogg, 2009; Eimer & Kiss, 2007, 2008; Woodman & Luck, 1999), to capture temporal differences within the N2pc effect. Specifically, in our case, the N2pc window our peak analysis approach selected was later than typically used to study the N2pc (Although our analysis suggested the window from 240 to 340 msec post stimuli onset, it is more common to study the N2pc in the 200–300 msec window; Luck, 2014). Thus, by choosing to split the N2pc into an early and late half, what is more normally reported as the N2pc was encompassed by our early window.

In both analyses, epochs were 30-Hz low-pass filtered and then baseline-corrected using a −200- to 0-msec prestimulus baseline period. To enable isolation of lateralized target-specific components, the reactive analysis consisted only of trials in which the target was presented on the horizontal midline, whereas the distractor was either absent or present on the vertical meridian—thereby evoking no lateralized component (Hickey, Di Lollo, & McDonald, 2009; Woodman & Luck, 2003). N2pc waveforms in the HP versus low-probability (LP) analysis were calculated over, on average, 61 trials per participant per condition, with a standard deviation of 13 trials. The stimuli features and arrangements were exactly identical in the HP and LP trials considered in the reactive analysis, differing only in their respective conditions (i.e., HP vs. LP). For the anticipatory analysis, because only fixation was present, all trials were included in the analysis. Waveforms evoked by the various search displays were collapsed across left and right visual hemifield and left and right electrodes to produce separate waveforms for contralateral and ipsilateral scalp regions. In the anticipatory analysis, the ipsilateral hemifield referred to the hemifield containing the HP target location. In the reactive analysis, ipsilateral referred to

the hemifield that contained the search target. Lateralized difference waveforms were then computed by subtracting the ipsilateral from contralateral waveforms. Importantly, in the reactive analysis, low probability targets were selected from all trials where the high probability location did not match the target location on that specific trial. Neutral trials were not included in neither ERP analysis as they represented the trials in which spatial priority was being unlearned and thus there was no clear a priori expectation on their evoked neural activity. Incorrect trials were also excluded, matching our behavioral analysis.

Statistics

Behavioral results were analyzed using simple paired *t* tests. Temporal frequency results were analyzed using a cluster permutation test, a method that corrects for multiple comparisons (Cohen, 2014; Maris & Oostenveld, 2007). We specifically used the MNE function *permutation_cluster_1samp_test* (Gramfort et al., 2014) on both the broadband power data and the averaged alpha channel data in separate analyses (Figure 2B and C, respectively). Clusters were identified as contiguous data points in which a *t* statistic exceeded the threshold corresponding to a *p* value of .05. A null distribution for the test statistic was found via a Monte Carlo randomization procedure, which shuffled condition labels across 1024 iterations. Significant clusters in the unpermuted data were identified as those in which the test statistic was larger than the 95th percentile of our simulated null distribution, thus approximating a two-tailed *t* test with an alpha of .05. All cluster permutation tests were done over the entire timeseries of data except the N2pc analysis in which case we were uninterested in clusters that occurred outside the expected N2pc window, and thus, only the data within the N2pc window of interest was included. The N2pc analysis used repeated-measures analyses of variance (ANOVAs) and *t* tests. To see whether the ipsilateral response was larger than the contralateral response in our window of interest (the N2pc), we had a clear prediction that an N2pc should be observed and thus a one-tailed *t* test was used. For the ERP latency analysis, a jackknife test (Kiesel, Miller, Jolicœur, & Brisson, 2008; Miller, Patterson, & Ulrich, 1998) was used to measure latency differences with 50% of peak amplitude latency taken as the point of interest.

RESULTS

Behavior

When limiting our HP trials to those on the horizontal midline, we observed the same HP location speedup as previously reported in Duncan and colleagues (2023), $t(21) = 7.832$, $p < .001$, $d = 1.67$ (Figure 1C and D). A repeated-measures ANOVA taking Target Location (high- vs. low-probability) and Distractor Presence (present vs. absent) as factors further showed both a significant effect of Target Location and Distractor Presence (both Fs > 50, ps $< .001$), but no interaction between the two, indicating that the probability cuing effect was the same irrespective of whether the distractor was present or not ($F < 1$).

As is typical in statistical learning paradigms, to ensure our statistical learning effect was not entirely driven by intertrial priming (Maljkovic & Nakayama, 1994), the main analysis was also done while excluding all repetition trials (~17% of total trials). This analysis yielded the same pattern of results, $t(21) = 7.896$, $p < .001$, $d = 1.68$ (note Figure 1C and D do not include repetition trials). However, intertrial priming effects are known to persist longer than immediate trial repetitions—the original priming of pop-out study by Maljkovic and Nakayama (1994) already showed that target feature repetitions can speed responses even when these repetitions are not immediately temporally adjacent. This is especially relevant in the current context given that, counter to typical probability cuing studies with one static high probability regions (e.g., Won & Jiang, 2015; Jiang, Swallow, Rosenbaum, & Herzig, 2013), enhancement was not reliably observed in the neutral blocks (see Duncan et al., 2023, Supplementary Figure 1 for the neutral block analysis for the current data). Therefore, in an exploratory linear mixed-model's analysis (Bates et al., 2015), where, in contrast to conventional ANOVA approaches, data are not averaged but grouped per participant, we examined whether our observed benefit at the high probability location could solely be explained by intertrial repetitions. Although this analysis showed that four trials in the past still influenced selection speed on the current trial,[3] confirming the potent influence of priming, overall RTs were reliably faster at high probability locations than low probability locations even after controlling for such priming effects ($\beta = 10.37$, $SE = 2.894$, $p < .001$). This strongly suggests that intertrial priming cannot be the sole driver of the current behavioral effect and the absence of an effect in the neutral blocks thus should be attributed to a lack of statistical power rather than a lack of learning.

Anticipatory Phase Results

Separate analyses on lateralized power were first done for ping and no-ping trials. Cluster-based analysis of the entire frequency range found no significant clusters in the broadband signal for either trial type when contrasting contra- and ipsilateral electrodes (Figure 2A and B). Furthermore, this analysis revealed no significant clusters when combining the two conditions (Figure 2D). A more targeted analysis of the alpha range in this combined condition similarly found no clusters of interest (Figure 2E, black line; significant clusters would have been indicated if present). Alpha is occasionally separated between high-frequency and low-frequency bands (Klimesch, 2012); in fact, Wang and colleagues (2019), found that alpha lateralization in response to statistical learning was primarily present in the lower alpha band (7–10 Hz). To rule out the possibility that our alpha band selection was obscuring real

lateralization, average alpha in the lower (7–10) and higher (10–13) frequency ranges were also independently tested for significance. Again, no significant clusters were found in either half of the alpha range (Figure 2E), suggesting statistically learned enhancement, unlike top–down enhancement, is not indexed by alpha lateralization. Finally, a Bayesian analysis comparing overall alpha lateralization during the anticipatory phase showed weak evidence for the null hypothesis ($BF_{10} = 2.49$), matching previously reported results (Ferrante et al., 2023).

Next, we examined whether the preparatory EEG signal contained ADAN and LDAP components; neural markers that are typically associated with top–down attentional enhancement (Kiss et al., 2008; Van der Stigchel, Heslenfeld, & Theeuwes, 2006; Eimer et al., 2002; Harter et al., 1989; Figures 3A and B). Traditionally, these two components are recorded after an informative fixation cue indicates which location in space a target will appear. Because no such informative cue was used in the current experiment, these components were instead yoked to the neutral fixation onset. As can be seen in Figure 3, contralateral and ipsilateral waveforms did not reliably differ from one another in neither the ADAN nor the LDAP windows of interest (both ts < 1; Figure 3C). Furthermore, a separate analysis of the ADAN component within ping trials (Figure 3A inset), as well as the LDAP analysis excluding ping trials (Figure 3C dotted line), both did not result in significant findings, $t(21) = 1.44$, $p = .165$ and $t < 1$, respectively. Together with the results of our alpha lateralization analysis, the current data thus provide no evidence that statistically learned attentional enhancement recruits the same underlying cognitive mechanisms as top–down attentional enhancement.

Reactive Phase Results

As visualized in Figure 3, targets presented at the high probability locations appeared to be accompanied by a larger N2pc at high relative to low probability locations. To test the reliability of this effect, as a first step, the component was measured as the mean amplitudes from 240- to 340-msec post stimulus and subsequently analyzed using a repeated-measures ANOVA with within-subject factors Target Condition (HP, low probability) and Hemifield (contralateral to target, ipsilateral to target). This analysis confirmed that the N2pc was reliable across conditions, main effect Hemifield: $F(1, 21) = 12.217$, $p = .002$, $\eta^2 = .068$. Pairwise comparisons between contralateral and ipsilateral waveforms yielded reliable differences in both high- and low-probability target conditions, $t(21) = 5.586$, $p < 001$, $d = 1.191$; $t(21) = 1.842$, $p = .04$, $d = 0.393$, respectively, one-tailed t tests. However, the apparent difference

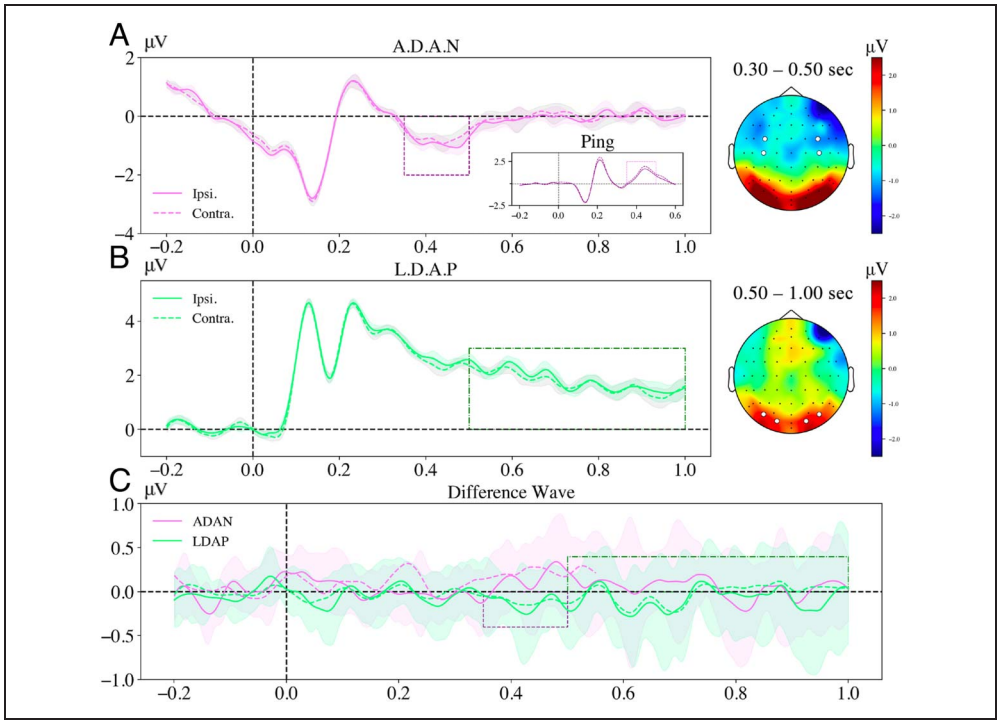

Figure 3. ADAN and LDAP preparatory ERP components following fixation onset in the intertrial period. All lines smoothed using the scipy Savitzky–Golay filter function (savgol_filter) with a polynomial order of 51 and a derivative of 3. (A) The ADAN component measured in the 300–500-msec window post fixation onset from electrodes C3/4 and FC3/4. Shaded area represents 95% confidence interval of mean using within-subject standard error calculated between ipsilateral and contralateral activity per participant (Cousineau, 2005). Full sensor array activity shown in the topography to the right (note: sensor space transformed such that the HP location was always on the right). Dotted box outlines window of interest. Shown in inset is evoked activity when yoked to ping onset on trials in which a ping occurred. Dotted gray line shows difference wave with gray shading indicating 95% confidence interval of mean. (B) The LDAP component measured from 500–1000 msec post fixation onset from the sensors PO7/8 and PO3/4. Full sensor array activity during time window of interest shown in topography on the right. (C) Difference waves for ADAN and LDAP analyses in time window up to 1 sec after fixation onset. Purple and green boxes represent the time windows of interest for ADAN and LDAP analyses, respectively. Shaded areas represent 95% confidence intervals of mean. Dotted green line represents average difference wave for LDAP sensors calculated on no-ping trials only. Dotted purple line represents the ADAN when Timepoint 0 represents the onset of a ping (50% of trials; search could onset at 600 msec post ping; thus, the line ends earlier than other conditions).

between targets at high and low probability locations was not reflected in a significant interaction, $F(1, 21) = 2.539, p = .126, \eta^2 = .004$.

Often the N2pc is separated into an early and a late window when visual inspection reveals distinct patterns of activity across the two halves (Eimer et al., 2010; Holmes et al., 2009; Eimer & Kiss, 2007, 2008; Woodman & Luck, 1999). Visual inspection of the respective difference waveforms suggested such a split may be informative in the current case as well; we therefore repeated the previous analyses separately for the early and the late parts of the N2pc component (240–290 msec and 290–340 msec post stimulus onset, respectively). These analyses again yielded reliable N2pcs across conditions (main effect hemifield: all Fs > 5.4, all ps $< .03$), but critically a significant interaction reflecting a more pronounced N2pc at high versus low-probability locations was only observed in the early time window, $F(1, 21) = 5.808, p = .025, \eta^2 = .009$. To further verify that a significant difference existed between our high- and low-probability conditions, a cluster-based permutation test was taken in our N2pc window of interest between the two continuous waveforms to test whether any significant clusters existed wherein the HP condition was reliably larger than the low-probability condition (see Methods section). A significant cluster was found in the early part of our early window of interest (Figure 4C; although the time course of cluster-based tests should be interpreted with caution, see Maris & Oostenveld, 2007). Finally, when the analysis was performed on a standard N2pc window (i.e., 200–300 msec), we again observed a reliable interaction, confirming that the N2pc amplitude reliably increased at high relative to low probability locations, $t(21) = 2.297, p = .032, d = 0.490$.

An additional analysis on the latency of the evoked N2pcs in HP and low-probability was also undertaken to see whether the behavioral speedup shown when targets appeared at HP locations was accompanied by a speeded neural response. Such decreased N2pc latencies have been shown in the past for both endogenous and exogenous cuing studies manipulating top–down attention (Foster et al., 2020; but see also Eimer & Kiss, 2008), but also when relative target salience was increased (Töllner et al., 2011). Using a jackknife procedure with a 50% peak (Ulrich & Miller, 2001), we found only anecdotal evidence for an N2pc onset difference, $t(21) = 1.753, p = .094$.

The observed N2pc modulation appears in line with a model in which statistical learning increases the perceived salience of targets at high probability target locations (Töllner et al., 2011). This conclusion however is premature, as the same pattern of results could also be

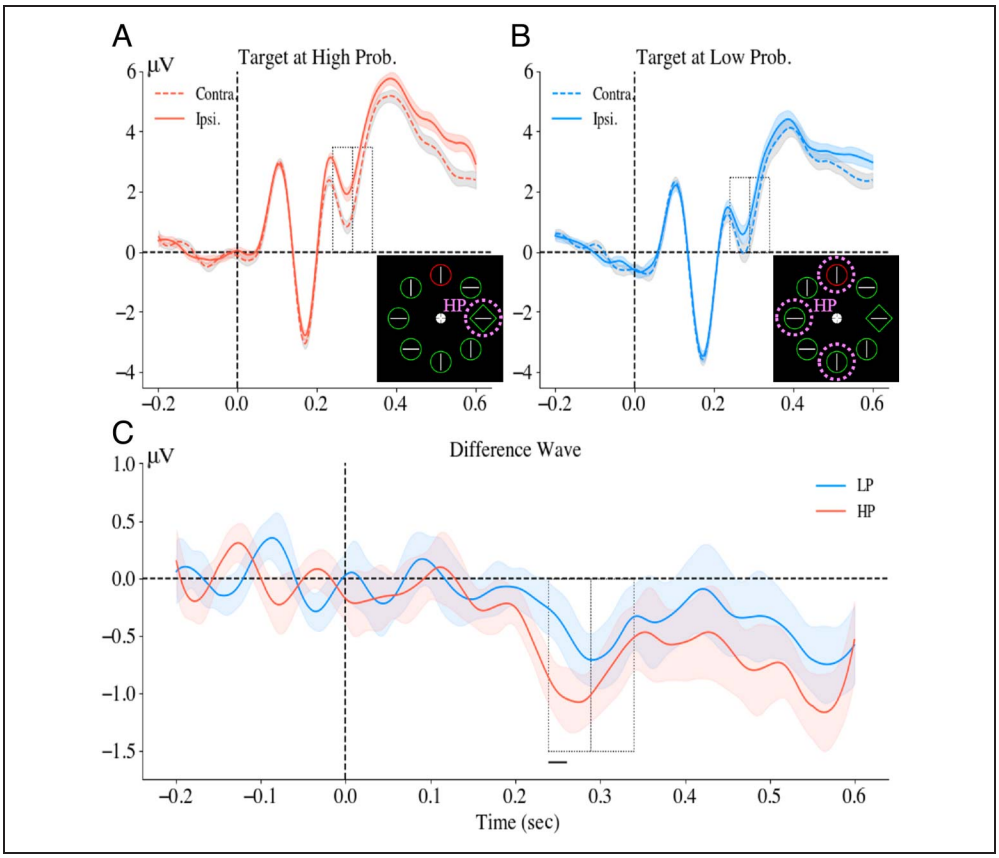

Figure 4. Grand averaged ERPs of electrodes of interest following search onset (vertical dotted black line) for HP (A) and LP (B) trials. In both figures, the solid line represents ipsilateral electrode activity, whereas the dotted lines represent contralateral activity. Trials pooled to generate these ERPs always held the target on the horizontal midline. Distractors could be present on the vertical meridian or were absent. (C) Difference waves calculated by subtracting contralateral from ipsilateral evoked activity for HP (red) and LP (blue) trials. Shaded areas represent the 95% confidence interval of the mean calculated using within-subject standard error measurements for each timepoint (Cousineau, 2005). The gray dotted box in each figure demarcates the N2pc window identified by the combined peak N2pc amplitude. The middle line represents the peak amplitude point, with the area to the left of the line being the early-N2pc window and to the right being the late-N2pc window. Black bars beneath waveforms in C represents significant cluster results of a one-sample cluster permutation test on the difference between HP and LP difference weaves within the N2pc window of interest. All lines smoothed using a Savitzky–Golay filter with a polynomial order of 51 and a derivative of 3.

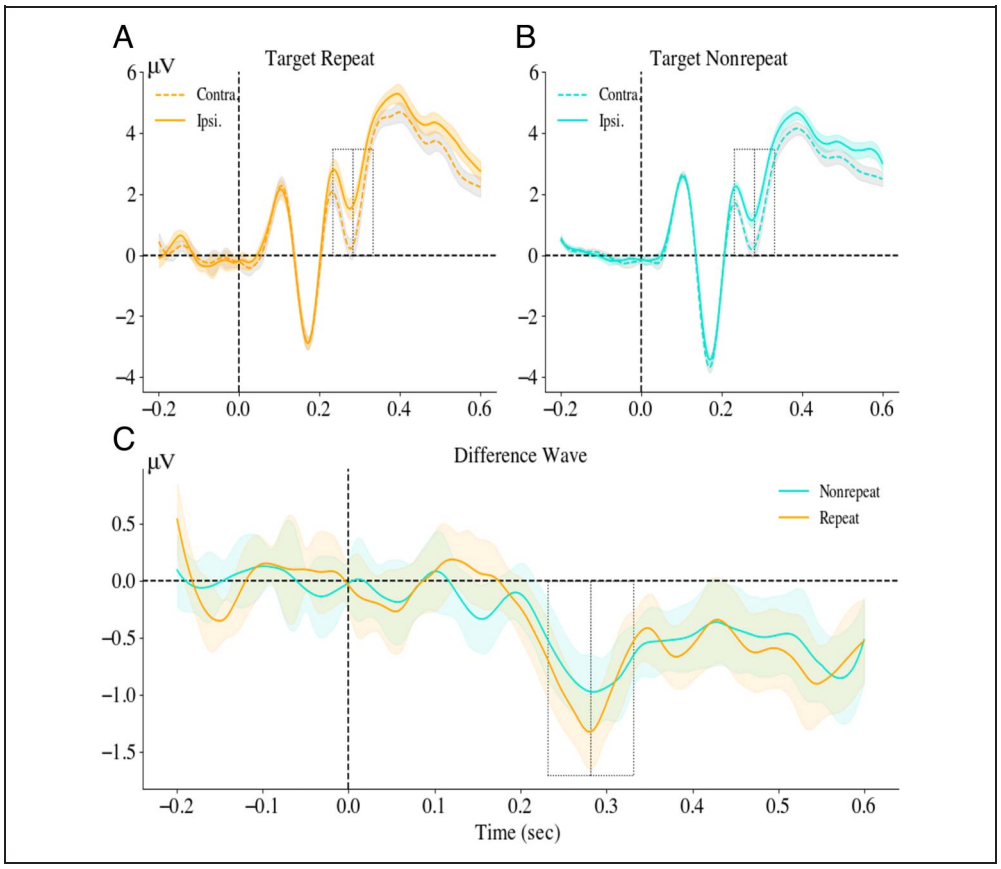

Figure 5. Grand averaged ERPs of electrodes of interest following search for trial in which the target was at the same location as the previous trial (repeat) (A) or at a different position (nonrepeat) (B). (C) Difference waves between contralateral and ipsilateral posterior electrodes. All shaded areas represent 95% confidence interval of mean using within-subject standard error scores. All lines were smoothed using a Savitzky–Golay filter with a polynomial order of 51 and a derivative of 3. In all figures, gray dotted box outlines N2pc window of interest with the middle line indicating combined peak amplitude and the left half of the box indicating the early-N2pc window and the right half the late N2pc window.

attributed to the fact that the high probability location has a higher proportion of target location repeats, a phenomenon that has been shown to result in an earlier onset of the N2pc (Eimer et al., 2010). Although we did not find a reliable shift in onset latency, the jackknife test was still close to significance, and it is thus possible that the observed amplitude modulation should be attributed to an earlier N2pc onset driven by intertrial priming. In an exploratory analysis, we therefore examined to what extent intertrial priming contributed to the observed pattern of results, by directly contrasting the waveforms elicited by targets at the horizontal midline (irrespective of the current condition: high or low probability) in trials where the target location repeated and trials in which the target location did not repeat. The rationale for this analysis being, if the results are primarily driven by intertrial priming, splitting the data in this way should result in an even larger condition difference than observed in the main analysis. As shown in Figure 5, however, although a robust N2pc was observed in both conditions, $F(1, 21) = 20.85$, $p < .001$, $\eta^2 = .21$, no interaction was found, neither in the early nor the whole N2pc window (all Fs < 1), indicating that the observed difference between N2pcs elicited at high and low probability locations should be contributed to statistical learning across longer time scales rather than intertrial priming. Furthermore, a jackknife analysis of the N2pc onsets between repeat and nonrepeat trials found no evidence of a speeded N2pc ($t < 1$), suggesting that spatial intertrial effects do not share the encephalographic characteristics of priming of pop out, where it has previously been shown that target feature repetitions exhibit a speeded N2pc response (Eimer et al., 2010).

DISCUSSION

Several studies have shown that visual search optimally adapts to the spatial probabilities underlying target presentation in a search task in a process known as statistical learning (Zhang et al., 2022; Jiang et al., 2013; Geng & Behrmann, 2002, 2005). The present study investigated both anticipatory and reactive encephalographic components to characterize the electrophysiological correlates of such statistically learned attentional enhancement. We modified the additional singleton paradigm (Theeuwes, 1991, 1992) such that targets appeared with higher probability at specific (yet periodically shifting) locations in the display. The data showed more efficient attentional selection of the target when presented at high relative to low probability target locations confirming earlier findings using this paradigm (Huang et al., 2022; Zhang et al., 2022; Gao & Theeuwes, 2020) and demonstrating that this learning also occurs when HP locations periodically shift during the experiment. The use of a shifting HP location as well as the lack of any carryover effects following the removal of target regularities motivated an additional

linear mixed-model analysis to tease apart how much of the observed behavioral effect was driven by statistical learning versus intertrial priming. While intertrial priming significantly contributed to our behavioral effect, it could not account for the entire speedup with a significant contribution attributed instead to statistical learning. It is important to note that although the current design was not properly optimized to study the extinction process of previous HP locations, the strong behavioral and encephalographic effects found indicate that the influence of previous learning blocks was marginal in comparison to the current HP location on any trial.

The encephalographic data were next separated into two phases—an anticipatory phase preceding the search display and reactive phase following it. Critically, although statistically learned attentional enhancement was neither characterized by anticipatory alpha lateralization nor by ADAN and LDAP components—preparatory encephalographic markers typically associated with top–down attention (Foster, Sutterer, Serences, Vogel, & Awh, 2017; Eimer & Kiss, 2008)—an exaggerated N2pc at high-relative to low-probability locations was found. Similar findings were found in studies in which target salience was varied (i.e., bottom–up attentional capture; Berggren & Eimer, 2020; Töllner et al., 2011; Mazza et al., 2009) and in studies investigating other selection history effects such as contextual cuing (Zinchenko, Conci, Töllner, Müller, & Geyer, 2020; Johnson, Woodman, Braun, & Luck, 2007) and value-driven capture (Hinault, Blacker, Gormley, Anderson, & Courtney, 2019; Kiss, Driver, & Eimer, 2009). Furthermore, intertrial priming could not be implicated as the main driver of this amplitude effect as an additional analysis focusing solely on repeat trials showed only a weak version of this effect, suggesting statistical learning as the main driver.

The lack of a contribution of markers associated with top–down attention indicates that statistically learned attentional enhancement utilizes neural mechanisms that are unlike those that are recruited during top–down attention. Although alpha lateralization in particular is a well-known marker of top–down attentional selection (Foster et al., 2017; Sauseng et al., 2005), it is unclear to what extent alpha lateralization is modulated by learning across longer time scales. Several studies have shown alpha lateralization in paradigms utilizing a form of statistically learned enhancement (van Moorselaar & Slagter, 2019; Noonan, Crittenden, Jensen, & Stokes, 2018); however, both of these studies explicitly cued the upcoming target location, either by directly cueing the upcoming static target location (Noonan et al., 2018) or by informing participants that the target location would repeat on consecutive trials (van Moorselaar and Slagter). Thus, their results arguably were a combination of both explicit top–down and statistically learned attentional enhancement. Interestingly, to date, there is in fact little evidence that alpha-band activity is modulated by spatial imbalances across displays (Ferrante et al., 2023; Qiu et al., 2023; van Moorselaar, Daneshtalab, & Slagter, 2021; van Moorselaar & Slagter, 2019; but see Wang et al., 2019). These studies however all examined alpha modulations in response to learning about distractor probabilities, leaving open the possibility that learning about probable target locations is reflected in anticipatory lateralized alpha band activity. Indeed, growing evidence suggests that alpha mediates direct enhancement of input at attended locations; rather than that, it suppresses irrelevant input as traditionally assumed (Jensen, 2023; Foster & Awh, 2019). However, the current results did not show reliable tuning within the alpha-band toward the HP target location, suggesting that learned attentional tuning is subserved by different neural mechanisms than top–down attentional orienting induced by endogenous cueing.

In further support of the tripartite model of attention first proposed by Awh and colleagues (2012), in which statistical learning is clearly distinct from top–down attention, the ADAN and LDAP components were also not lateralized relative to the high probability target locations. It is important to note however that the absence of these anticipatory components is not conclusive evidence that statistically learned attentional enhancement is not proactive in nature. In fact, ample behavioral evidence suggests that statistical learning effects can be implemented proactively (Huang et al., 2022; Huang, Vilotijević, Theeuwes, & Donk, 2021)—although these effects might be stimulus and task specific (Addleman, Schmidt, Remington, & Jiang, 2019; Addleman, Tao, Remington, & Jiang, 2018). Rather, the current evidence is consistent with the recently proposed synaptic model of statistical learning (Duncan et al., 2023; Ferrante et al., 2023; van Moorselaar et al., 2020). In the work of Ferrante and colleagues (2023), it was shown that although statistical learning (in their case of distractor regularities) did not lead to alpha lateralization, it did lead to reduced neural excitability in the suppressed hemifield, as indexed by frequency tagging. Ferrante and colleagues (2023) argue that this reduced excitability may be evidence for a latent synaptic mechanism, suppressing excitability of spatially tuned neurons in suppressed regions, but not resulting in the activity necessary to see alpha lateralization. Such a reduction in excitability of spatially tuned neurons may then lead to attenuated saliency signals from the suppressed region in space, leading to their reduced distractor interference. This down-weighting of space on the latent spatial priority map would then represent the opposite effect as what has been reported here: an upweighting of saliency signals for targets presented at enhanced locations in space. It is important to note that just as in the Ferrante and colleagues (2023) study, the current data are also in line with the idea that the priority landscape, although seemingly only apparent after search display onset, was already in place before search display onset. As reported in Duncan and colleagues (2023), multivariate analyses yoked to the neutral pings presented on half of the trials before search display onset revealed the anticipatory priority landscape. It thus appears that

although statistical learning proactively adjusts the spatial priority map, this priority landscape only becomes apparent after integration of bottom–up sensory input (van Moorselaar & Slagter, 2020) such as a probe display (Huang et al., 2021, 2022), a placeholder display (Ferrante et al., 2023) or a task irrelevant perturbation (Duncan et al., 2023), or as reported here the onset of the actual search display.

The examination of the reactive ERP components in the current data set revealed a novel finding that early N2pc amplitude increases when targets are presented in HP locations, a finding that importantly has not been observed in response to top–down orienting of attention (Foster et al., 2020; Kiss et al., 2008). Although traditionally it was believed that the N2pc reflected attentional selection (Woodman & Luck, 1999; Eimer, 1996), more recently, it was proposed that this component may in fact track target individuation from background distractors (Mazza & Caramazza, 2015; Mazza, Pagano, & Caramazza, 2013; Pagano & Mazza, 2012; Mazza et al., 2009). Following this reasoning, we take our findings to reflect that targets are perceived as more salient at high probability locations. Consistent with this, in a series of experiments, Töllner and colleagues (2011) showed that systematic increases of target salience (orientation or color) relative to background elements led to a monotonic increase in the subsequent N2pc amplitude. Töllner et al. concluded that the N2pc amplitude is effectively an indication of relative target salience, reflecting the ease in which targets are individuated from background elements (Töllner et al., 2011; for similar findings, see Berggren & Eimer, 2020; Zhao et al., 2011; Mazza et al., 2009).[4] In the current study, search displays were exactly identical between HP and low-probability trials, with the only difference being the learning manipulation. The heightened N2pc observed in the current study thus reflects an upweighting of saliency information at the learned HP target location, a result consistent with the aforementioned latent excitability account. Increased saliency should then result in stronger pop-out effects during parallel search, accounting for the widely reported probability cuing effect. Importantly, exogenous (bottom–up) attention shifts (via lateral abrupt visual or audio onsets) has also been shown to affect the physical appearance of items (termed "perceived salience"; Störmer, McDonald, & Hillyard, 2009; Carrasco, Ling, & Read, 2004; for a review, see Carrasco & Barbot, 2019). Therefore, the current encephalographic results seem to suggest that learned attentional enhancement may boost and sharpen its spatial representation in a similar way as exogenous (bottom–up) shifts of attention (see Theeuwes, 2018, for similar arguments).

Furthermore, although the current study is the first to report an amplitude effect in a probability cuing paradigm, it is not the first to observe an amplitude effect in response to selection history effects. Although selection history is a broad category of behavioral effects, numerous studies on different forms of selection history bias have found that the behavioral benefits of target processing are accompanied by an exaggerated N2pc. These include contextual cuing paradigms (Zinchenko et al., 2020; Schankin & Schubö, 2010; Johnson et al., 2007; Olson, Chun, & Allison, 2001) and value-driven capture paradigms (Hinault et al., 2019; MacLean & Giesbrecht, 2015; Qi, Zeng, Ding, & Li, 2013; Kiss et al., 2009), two version of selection history effects that are necessarily reactive in nature. The current addition of selection history to this list begins to advocate for a consensus that N2pc modulations are a general marker of selection history effects.[5]

Acknowledgments

This research was supported by a European Research Council advanced grant 833029 – [LEARNATTEND].

Reprint requests should be sent to D. H. Duncan, Department of Experimental and Applied Psychology, Vrije Universiteit Amsterdam, Van der Boechorststraat 7, 1081 BT Amsterdam, The Netherlands, or via e-mail: D.H.Duncan@vu.nl.

Data Availability Statement

All anonymized participant EEG, eye tracking, and behavioral data are available online at: https://osf.io/v7yhc/.

Author Contributions

Original idea by D. H. D., J. T., and D. v. M. Experiment programmed by D. H. D. and D. v. M. Data collected by D. H. D. Analysis programmed by D. H. D. and D. v. M. Manuscript drafted and revised by D. H. D., J. T., and D. v. M.

Funding Information

H2020 European Research Council (https://dx.doi.org/10.13039/100010663), grant number: 833029 – [LEARNATTEND].

Diversity in Citation Practices

Retrospective analysis of the citations in every article published in this journal from 2010 to 2021 reveals a persistent pattern of gender imbalance: Although the proportions of authorship teams (categorized by estimated gender identification of first author/last author) publishing in the *Journal of Cognitive Neuroscience* (*JoCN*) during this period were M(an)/M = .407, W(oman)/M = .32, M/W = .115, and W/W = .159, the comparable proportions for the articles that these authorship teams cited were M/M = .549, W/M = .257, M/W = .109, and W/W = .085 (Postle and Fulvio, *JoCN*, 34:1, pp. 1–3). Consequently, *JoCN* encourages all authors to consider gender balance explicitly when selecting which articles to cite and gives them the opportunity to report their article's gender citation balance.

Notes

1. The two excluded participants had HP presentation orders of [left, bottom, right, top] and [right, bottom, left, top].
2. Note that the reported analysis (using five back trials) was the first analysis undertaken, and model comparisons showed no improvement by adding further trial-back conditions.
3. For model parameters, see Methods section. Statistics for intertrial priming effects: 1-back ($\beta = 19.48$, $SE = 4.440$, $p < .001$); 2-back ($\beta = 12.66$, $SE = 3.118$, $p < .001$); 3-back ($\beta = 8.065$, $SE = 2.982$, $p < .01$); 4-back ($\beta = 8.636$, $SE = 3.326$, $p < .05$); 5-back ($\beta = 4.321$, $SE = 3.045$, $p = .158$). Note that linear mixed models regress out the relative contribution of each effect such that each reported effect is independent.
4. Note that Töllner and colleagues (2011) also showed a reliable speedup of the N2pc as saliency scaled, a result that, in the current data, was only anecdotally present.
5. Interestingly, a very recent study by Dolci and colleagues (2023) studied a version of the probability cuing paradigm using serial search and found that rather than an N2pc amplitude modulation, the N2pc reversed such that it seemed attention was initially captured by neutral distractors at the high-probability location. Because their task required serial search, it is likely that this difference stems from a reduced role of saliency in their task. In our task, processing occurs in parallel across all display items and attention is orientated toward the most salient item within the display. In the Dolci and colleagues (2023) task, search was likely serially directed toward the high-probability location irrespective of the stimuli's bottom–up saliency. As a result, attention may have been directed toward items at the high-probability location regardless of their bottom–up characteristics.

REFERENCES

Addleman, D. A., Schmidt, A. L., Remington, R. W., & Jiang, Y. V. (2019). Implicit location probability learning does not induce baseline shifts of visuospatial attention. *Psychonomic Bulletin & Review*, *26*, 552–558. https://doi.org/10.3758/s13423-019-01588-8, PubMed: 30887446

Addleman, D. A., Tao, J., Remington, R. W., & Jiang, Y. V. (2018). Explicit goal-driven attention, unlike implicitly learned attention, spreads to secondary tasks. *Journal of Experimental Psychology: Human Perception and Performance*, *44*, 356–366. https://doi.org/10.1037/xhp0000457, PubMed: 28795835

Anderson, B. A., Kim, H., Kim, A. J., Liao, M.-R., Mrkonja, L., Clement, A., et al. (2021). The past, present, and future of selection history. *Neuroscience & Biobehavioral Reviews*, *130*, 326–350. https://doi.org/10.1016/j.neubiorev.2021.09.004, PubMed: 34499927

Awh, E., Belopolsky, A. V., & Theeuwes, J. (2012). Top–down versus bottom–up attentional control: A failed theoretical dichotomy. *Trends in Cognitive Sciences*, *16*, 437–443. https://doi.org/10.1016/j.tics.2012.06.010, PubMed: 22795563

Bates, D., Mächler, M., Bolker, B., & Walker, S. (2015). Fitting linear mixed-effects models using lme4. *Journal of Statistical Software*, *67*, 1–48. https://doi.org/10.18637/jss.v067.i01

Berggren, N., & Eimer, M. (2020). Spatial filtering restricts the attentional window during both singleton and feature-based visual search. *Attention, Perception, & Psychophysics*, *82*, 2360–2378. https://doi.org/10.3758/s13414-020-01977-5, PubMed: 31993978

Britton, M. K., & Anderson, B. A. (2020). Specificity and persistence of statistical learning in distractor suppression. *Journal of Experimental Psychology: Human Perception and Performance*, *46*, 324–334. https://doi.org/10.1037/xhp0000718, PubMed: 31886698

Carrasco, M., & Barbot, A. (2019). Spatial attention alters visual appearance. *Current Opinion in Psychology*, *29*, 56–64. https://doi.org/10.1016/j.copsyc.2018.10.010, PubMed: 30572280

Carrasco, M., Ling, S., & Read, S. (2004). Attention alters appearance. *Nature Neuroscience*, *7*, 308–313. https://doi.org/10.1038/nn1194, PubMed: 14966522

Cohen, M. X. (2014). *Analyzing neural time series data: Theory and practice*. Cambridge, MA: MIT Press. https://doi.org/10.7551/mitpress/9609.001.0001

Cousineau, D. (2005). Confidence intervals in within-subject designs: A simpler solution to Loftus and Masson's method. *Tutorials in Quantitative Methods for Psychology*, *1*, 42–45. https://doi.org/10.20982/tqmp.01.1.p042

Desimone, R., & Duncan, J. (1995). Neural mechanisms of selective visual attention. *Annual Review of Neuroscience*, *18*, 193–222. https://doi.org/10.1146/annurev.ne.18.030195.001205, PubMed: 7605061

de Vries, I. E. J., van Driel, J., & Olivers, C. N. L. (2017). Posterior α EEG dynamics dissociate current from future goals in working memory-guided visual search. *Journal of Neuroscience*, *37*, 1591–1603. https://doi.org/10.1523/JNEUROSCI.2945-16.2016, PubMed: 28069918

Dolci, C., Boehler, C. N., Santandrea, E., Dewulf, A., Ben-Hamed, S., Macaluso, E., et al. (2023). Integrated effects of top–down attention and statistical learning during visual search: An EEG study. *Attention, Perception, & Psychophysics*, *85*, 1819–1833. https://doi.org/10.3758/s13414-023-02728-y, PubMed: 37264294

Duncan, D. H., & Theeuwes, J. (2020). Statistical learning in the absence of explicit top–down attention. *Cortex*, *131*, 54–65. https://doi.org/10.1016/j.cortex.2020.07.006, PubMed: 32801075

Duncan, D. H., van Moorselaar, D., & Theeuwes, J. (2023). Pinging the brain to reveal the hidden attentional priority map using encephalography. *Nature Communications*, *14*, 4749. https://doi.org/10.1038/s41467-023-40405-8, PubMed: 37550310

Egeth, H. E., & Yantis, S. (1997). Visual attention: Control, representation, and time course. *Annual Review of Psychology*, *48*, 269–297. https://doi.org/10.1146/annurev.psych.48.1.269, PubMed: 9046562

Eimer, M. (1996). The N2pc component as an indicator of attentional selectivity. *Electroencephalography and Clinical Neurophysiology*, *99*, 225–234. https://doi.org/10.1016/0013-4694(96)95711-9, PubMed: 8862112

Eimer, M., & Kiss, M. (2007). Attentional capture by task-irrelevant fearful faces is revealed by the N2pc component. *Biological Psychology*, *74*, 108–112. https://doi.org/10.1016/j.biopsycho.2006.06.008, PubMed: 16899334

Eimer, M., & Kiss, M. (2008). Involuntary attentional capture is determined by task set: Evidence from event-related brain potentials. *Journal of Cognitive Neuroscience*, *20*, 1423–1433. https://doi.org/10.1162/jocn.2008.20099, PubMed: 18303979

Eimer, M., Kiss, M., & Cheung, T. (2010). Priming of pop-out modulates attentional target selection in visual search: Behavioural and electrophysiological evidence. *Vision Research*, *50*, 1353–1361. https://doi.org/10.1016/j.visres.2009.11.001, PubMed: 19895829

Eimer, M., van Velzen, J., & Driver, J. (2002). Cross-modal interactions between audition, touch, and vision in endogenous spatial attention: ERP evidence on preparatory states and sensory modulations. *Journal of Cognitive Neuroscience*, *14*, 254–271. https://doi.org/10.1162/089892902317236885, PubMed: 11970790

Failing, M., & Theeuwes, J. (2018). Selection history: How reward modulates selectivity of visual attention. *Psychonomic Bulletin & Review*, *25*, 514–538. https://doi.org/10.3758/s13423-017-1380-y, PubMed: 28986770

Fecteau, J. H., & Munoz, D. P. (2006). Salience, relevance, and firing: A priority map for target selection. *Trends in Cognitive Sciences*, *10*, 382–390. https://doi.org/10.1016/j.tics.2006.06.011, PubMed: 16843702

Ferrante, O., Patacca, A., Di Caro, V., Della Libera, C., Santandrea, E., & Chelazzi, L. (2018). Altering spatial priority maps via statistical learning of target selection and distractor filtering. *Cortex*, *102*, 67–95. https://doi.org/10.1016/j.cortex.2017.09.027, PubMed: 29096874

Ferrante, O., Zhigalov, A., Hickey, C., & Jensen, O. (2023). Statistical learning of distractor suppression downregulates prestimulus neural excitability in early visual cortex. *Journal of Neuroscience*, *43*, 2190–2198. https://doi.org/10.1523/JNEUROSCI.1703-22.2022, PubMed: 36801825

Foster, J. J., & Awh, E. (2019). The role of alpha oscillations in spatial attention: Limited evidence for a suppression account. *Current Opinion in Psychology*, *29*, 34–40. https://doi.org/10.1016/j.copsyc.2018.11.001, PubMed: 30472541

Foster, J. J., Bsales, E. M., & Awh, E. (2020). Covert spatial attention speeds target individuation. *Journal of Neuroscience*, *40*, 2717–2726. https://doi.org/10.1523/JNEUROSCI.2962-19.2020, PubMed: 32054678

Foster, J. J., Sutterer, D. W., Serences, J. T., Vogel, E. K., & Awh, E. (2017). Alpha-band oscillations enable spatially and temporally resolved tracking of covert spatial attention. *Psychological Science*, *28*, 929–941. https://doi.org/10.1177/0956797617699167, PubMed: 28537480

Gao, Y., & Theeuwes, J. (2020). Independent effects of statistical learning and top–down attention. *Attention, Perception, & Psychophysics*, *82*, 3895–3906. https://doi.org/10.3758/s13414-020-02115-x, PubMed: 32909086

Geng, J. J., & Behrmann, M. (2002). Probability cuing of target location facilitates visual search implicitly in normal participants and patients with hemispatial neglect. *Psychological Science*, *13*, 520–525. https://doi.org/10.1111/1467-9280.00491, PubMed: 12430835

Geng, J. J., & Behrmann, M. (2005). Spatial probability as an attentional cue in visual search. *Perception & Psychophysics*, *67*, 1252–1268. https://doi.org/10.3758/BF03193557, PubMed: 16502846

Gramfort, A., Luessi, M., Larson, E., Engemann, D. A., Strohmeier, D., Brodbeck, C., et al. (2014). MNE software for processing MEG and EEG data. *Neuroimage*, *86*, 446–460. https://doi.org/10.1016/j.neuroimage.2013.10.027, PubMed: 24161808

Harter, M. R., Miller, S. L., Price, N. J., LaLonde, M. E., & Keyes, A. L. (1989). Neural processes involved in directing attention. *Journal of Cognitive Neuroscience*, *1*, 223–237. https://doi.org/10.1162/jocn.1989.1.3.223, PubMed: 23968506

Hickey, C., Di Lollo, V., & McDonald, J. J. (2009). Electrophysiological indices of target and distractor processing in visual search. *Journal of Cognitive Neuroscience*, *21*, 760–775. https://doi.org/10.1162/jocn.2009.21039, PubMed: 18564048

Hinault, T., Blacker, K. J., Gormley, M., Anderson, B. A., & Courtney, S. M. (2019). Value-driven attentional capture is modulated by the contents of working memory: An EEG study. *Cognitive, Affective, & Behavioral Neuroscience*, *19*, 253–267. https://doi.org/10.3758/s13415-018-00663-2, PubMed: 30460482

Holmes, A., Bradley, B. P., Nielsen, M. K., & Mogg, K. (2009). Attentional selectivity for emotional faces: Evidence from human electrophysiology. *Psychophysiology*, *46*, 62–68. https://doi.org/10.1111/j.1469-8986.2008.00750.x, PubMed: 19055500

Huang, C., Donk, M., & Theeuwes, J. (2022). Proactive enhancement and suppression elicited by statistical regularities in visual search. *Journal of Experimental Psychology: Human Perception and Performance*, *48*, 443–457. https://doi.org/10.1037/xhp0001002, PubMed: 35324244

Huang, C., Vilotijević, A., Theeuwes, J., & Donk, M. (2021). Proactive distractor suppression elicited by statistical regularities in visual search. *Psychonomic Bulletin & Review*, *28*, 918–927. https://doi.org/10.3758/s13423-021-01891-3, PubMed: 33620698

Jensen, O. (2023). Gating by alpha band inhibition revised: A case for a secondary control mechanism. *PsyArXiv*. https://doi.org/10.31234/osf.io/7bk32

Jiang, Y. V. (2018). Habitual versus goal-driven attention. *Cortex*, *102*, 107–120. https://doi.org/10.1016/j.cortex.2017.06.018, PubMed: 28734549

Jiang, Y. V., Swallow, K. M., Rosenbaum, G. M., & Herzig, C. (2013). Rapid acquisition but slow extinction of an attentional bias in space. *Journal of Experimental Psychology: Human Perception and Performance*, *39*, 87–99. https://doi.org/10.1037/a0027611, PubMed: 22428675

Johnson, J. S., Woodman, G. F., Braun, E., & Luck, S. J. (2007). Implicit memory influences the allocation of attention in visual cortex. *Psychonomic Bulletin & Review*, *14*, 834–839. https://doi.org/10.3758/BF03194108, PubMed: 18087946

Kiesel, A., Miller, J., Jolicœur, P., & Brisson, B. (2008). Measurement of ERP latency differences: A comparison of single-participant and jackknife-based scoring methods. *Psychophysiology*, *45*, 250–274. https://doi.org/10.1111/j.1469-8986.2007.00618.x, PubMed: 17995913

Kiss, M., Driver, J., & Eimer, M. (2009). Reward priority of visual target singletons modulates event-related potential signatures of attentional selection. *Psychological Science*, *20*, 245–251. https://doi.org/10.1111/j.1467-9280.2009.02281.x, PubMed: 19175756

Kiss, M., Van Velzen, J., & Eimer, M. (2008). The N2pc component and its links to attention shifts and spatially selective visual processing. *Psychophysiology*, *45*, 240–249. https://doi.org/10.1111/j.1469-8986.2007.00611.x, PubMed: 17971061

Klimesch, W. (2012). Alpha-band oscillations, attention, and controlled access to stored information. *Trends in Cognitive Sciences*, *16*, 606–617. https://doi.org/10.1016/j.tics.2012.10.007, PubMed: 23141428

Koch, C., & Ullman, S. (1984). Selecting one among the many: A simple network implementing shifts in selective visual attention (Tech Rep. No. AIM-770). MIT Press.

Luck, S. J. (2014). *An introduction to the event-related potential technique* (2nd ed.). Cambridge, MA: MIT Press.

Luck, S. J., Gaspelin, N., Folk, C. L., Remington, R. W., & Theeuwes, J. (2021). Progress toward resolving the attentional capture debate. *Visual Cognition*, *29*, 1–21. https://doi.org/10.1080/13506285.2020.1848949, PubMed: 33574729

Luck, S. J., & Hillyard, S. A. (1994). Spatial filtering during visual search: Evidence from human electrophysiology. *Journal of Experimental Psychology: Human Perception and Performance*, *20*, 1000–1014. https://doi.org/10.1037/0096-1523.20.5.1000, PubMed: 7964526

MacLean, M. H., & Giesbrecht, B. (2015). Neural evidence reveals the rapid effects of reward history on selective attention. *Brain Research*, *1606*, 86–94. https://doi.org/10.1016/j.brainres.2015.02.016, PubMed: 25701717

Maljkovic, V., & Nakayama, K. (1994). Priming of pop-out: I. Role of features. *Memory & Cognition*, *22*, 657–672. https://doi.org/10.3758/BF03209251, PubMed: 7808275

Maris, E., & Oostenveld, R. (2007). Nonparametric statistical testing of EEG-and MEG-data. *Journal of Neuroscience*

Methods, *164*, 177–190. https://doi.org/10.1016/j.jneumeth.2007.03.024, PubMed: 17517438
Mathôt, S., Schreij, D., & Theeuwes, J. (2012). OpenSesame: An open-source, graphical experiment builder for the social sciences. *Behavior Research Methods*, *44*, 314–324. https://doi.org/10.3758/s13428-011-0168-7, PubMed: 22083660
Mazza, V., & Caramazza, A. (2015). Multiple object individuation and subitizing in enumeration: A view from electrophysiology. *Frontiers in Human Neuroscience*, *9*, 162. https://doi.org/10.3389/fnhum.2015.00162, PubMed: 25883563
Mazza, V., Pagano, S., & Caramazza, A. (2013). Multiple object individuation and exact enumeration. *Journal of Cognitive Neuroscience*, *25*, 697–705. https://doi.org/10.1162/jocn_a_00349, PubMed: 23249353
Mazza, V., Turatto, M., & Caramazza, A. (2009). Attention selection, distractor suppression and N2pc. *Cortex*, *45*, 879–890. https://doi.org/10.1016/j.cortex.2008.10.009, PubMed: 19084218
Miller, J., Patterson, T., & Ulrich, R. (1998). Jackknife-based method for measuring LRP onset latency differences. *Psychophysiology*, *35*, 99–115. https://doi.org/10.1111/1469-8986.3510099, PubMed: 9499711
Murray, A. M., Nobre, A. C., & Stokes, M. G. (2011). Markers of preparatory attention predict visual short-term memory performance. *Neuropsychologia*, *49*, 1458–1465. https://doi.org/10.1016/j.neuropsychologia.2011.02.016, PubMed: 21335015
Myers, N. E., Walther, L., Wallis, G., Stokes, M. G., & Nobre, A. C. (2015). Temporal dynamics of attention during encoding versus maintenance of working memory: Complementary views from event-related potentials and alpha-band oscillations. *Journal of Cognitive Neuroscience*, *27*, 492–508. https://doi.org/10.1162/jocn_a_00727, PubMed: 25244118
Nobre, A. C., Sebestyen, G. N., & Miniussi, C. (2000). The dynamics of shifting visuospatial attention revealed by event-related potentials. *Neuropsychologia*, *38*, 964–974. https://doi.org/10.1016/S0028-3932(00)00015-4, PubMed: 10775707
Noonan, M. P., Crittenden, B. M., Jensen, O., & Stokes, M. G. (2018). Selective inhibition of distracting input. *Behavioural Brain Research*, *355*, 36–47. https://doi.org/10.1016/j.bbr.2017.10.010, PubMed: 29042157
Olson, I. R., Chun, M. M., & Allison, T. (2001). Contextual guidance of attention: Human intracranial event-related potential evidence for feedback modulation in anatomically early temporally late stages of visual processing. *Brain*, *124*, 1417–1425. https://doi.org/10.1093/brain/124.7.1417, PubMed: 11408336
Oostenveld, R., Fries, P., Maris, E., & Schoffelen, J.-M. (2011). FieldTrip: Open source software for advanced analysis of MEG, EEG, and invasive electrophysiological data. *Computational Intelligence and Neuroscience*, *2011*, 156869. https://doi.org/10.1155/2011/156869, PubMed: 21253357
Pagano, S., & Mazza, V. (2012). Individuation of multiple targets during visual enumeration: New insights from electrophysiology. *Neuropsychologia*, *50*, 754–761. https://doi.org/10.1016/j.neuropsychologia.2012.01.009, PubMed: 22266261
Perrin, F., Pernier, J., Bertrand, O., & Echallier, J. F. (1989). Spherical splines for scalp potential and current density mapping. *Electroencephalography and Clinical Neurophysiology*, *72*, 184–187. https://doi.org/10.1016/0013-4694(89)90180-6, PubMed: 2464490
Peirce, J. W. (2007). PsychoPy—Psychophysics software in python. *Journal of Neuroscience Methods*, *162*, 8–13. https://doi.org/10.1016/j.jneumeth.2006.11.017, PubMed: 17254636
Qi, S., Zeng, Q., Ding, C., & Li, H. (2013). Neural correlates of reward-driven attentional capture in visual search. *Brain Research*, *1532*, 32–43. https://doi.org/10.1016/j.brainres.2013.07.044, PubMed: 23916733
Qiu, N., Zhang, B., Allenmark, F., Nasemann, J., Tsai, S.-Y., Müller, H. J., et al. (2023). Long-term (statistically learnt) and short-term (inter-trial) distractor-location effects arise at different pre- and post-selective processing stages. *Psychophysiology*, *60*, e14351. https://doi.org/10.1111/psyp.14351, PubMed: 37277926
Rihs, T. A., Michel, C. M., & Thut, G. (2007). Mechanisms of selective inhibition in visual spatial attention are indexed by α-band EEG synchronization. *European Journal of Neuroscience*, *25*, 603–610. https://doi.org/10.1111/j.1460-9568.2007.05278.x, PubMed: 17284203
Sauseng, P., Klimesch, W., Stadler, W., Schabus, M., Doppelmayr, M., Hanslmayr, S., et al. (2005). A shift of visual spatial attention is selectively associated with human EEG alpha activity. *European Journal of Neuroscience*, *22*, 2917–2926. https://doi.org/10.1111/j.1460-9568.2005.04482.x, PubMed: 16324126
Schankin, A., & Schubö, A. (2010). Contextual cueing effects despite spatially cued target locations. *Psychophysiology*, *47*, 717–727. https://doi.org/10.1111/j.1469-8986.2010.00979.x, PubMed: 20230499
Störmer, V. S., McDonald, J. J., & Hillyard, S. A. (2009). Cross-modal cueing of attention alters appearance and early cortical processing of visual stimuli. *Proceedings of the National Academy of Sciences, U.S.A.*, *106*, 22456–22461. https://doi.org/10.1073/pnas.0907573106, PubMed: 20007778
Thaler, L., Schütz, A. C., Goodale, M. A., & Gegenfurtner, K. R. (2013). What is the best fixation target? The effect of target shape on stability of fixational eye movements. *Vision Research*, *76*, 31–42. https://doi.org/10.1016/j.visres.2012.10.012, PubMed: 23099046
Theeuwes, J. (1991). Cross-dimensional perceptual selectivity. *Perception & Psychophysics*, *50*, 184–193. https://doi.org/10.3758/BF03212219, PubMed: 1945740
Theeuwes, J. (1992). Perceptual selectivity for color and form. *Perception & Psychophysics*, *51*, 599–606. https://doi.org/10.3758/BF03211656, PubMed: 1620571
Theeuwes, J. (2010). Top–down and bottom–up control of visual selection. *Acta Psychologica*, *135*, 77–99. https://doi.org/10.1016/j.actpsy.2010.02.006, PubMed: 20507828
Theeuwes, J. (2018). Visual selection: Usually fast and automatic; seldom slow and volitional. *Journal of Cognition*, *1*, 29. https://doi.org/10.5334/joc.13, PubMed: 31517202
Theeuwes, J. (2019). Goal-driven, stimulus-driven, and history-driven selection. *Current Opinion in Psychology*, *29*, 97–101. https://doi.org/10.1016/j.copsyc.2018.12.024, PubMed: 30711911
Theeuwes, J., Bogaerts, L., & van Moorselaar, D. (2022). What to expect where and when: How statistical learning drives visual selection. *Trends in Cognitive Sciences*, *26*, 860–872. https://doi.org/10.1016/j.tics.2022.06.001, PubMed: 35840476
Töllner, T., Zehetleitner, M., Gramann, K., & Müller, H. J. (2011). Stimulus saliency modulates pre-attentive processing speed in human visual cortex. *PLoS One*, *6*, e16276. https://doi.org/10.1371/journal.pone.0016276, PubMed: 21283699
Ulrich, R., & Miller, J. (2001). Using the jackknife-based scoring method for measuring LRP onset effects in factorial designs. *Psychophysiology*, *38*, 816–827. https://doi.org/10.1111/1469-8986.3850816, PubMed: 11577905
Valsecchi, M., & Turatto, M. (2021). Distractor filtering is affected by local and global distractor probability, emerges very rapidly but is resistant to extinction. *Attention, Perception, & Psychophysics*, *83*, 2458–2472. https://doi.org/10.3758/s13414-021-02303-3, PubMed: 33948881

Van der Stigchel, S., Heslenfeld, D. J., & Theeuwes, J. (2006). An ERP study of preparatory and inhibitory mechanisms in a cued saccade task. *Brain Research*, *1105*, 32–45. https://doi.org/10.1016/j.brainres.2006.02.089, PubMed: 16595127

van Moorselaar, D., Daneshtalab, N., & Slagter, H. A. (2021). Neural mechanisms underlying distractor inhibition on the basis of feature and/or spatial expectations. *Cortex*, *137*, 232–250. https://doi.org/10.1016/j.cortex.2021.01.010, PubMed: 33640854

van Moorselaar, D., Lampers, E., Cordesius, E., & Slagter, H. A. (2020). Neural mechanisms underlying expectation-dependent inhibition of distracting information. *eLife*, *9*, e61048. https://doi.org/10.7554/eLife.61048, PubMed: 33320084

van Moorselaar, D., & Slagter, H. A. (2019). Learning what is irrelevant or relevant: Expectations facilitate distractor inhibition and target facilitation through distinct neural mechanisms. *Journal of Neuroscience*, *39*, 6953–6967. https://doi.org/10.1523/JNEUROSCI.0593-19.2019, PubMed: 31270162

van Moorselaar, D., & Slagter, H. A. (2020). Inhibition in selective attention. *Annals of the New York Academy of Sciences*, *1464*, 204–221. https://doi.org/10.1111/nyas.14304, PubMed: 31951294

Wagenmakers, E.-J., Love, J., Marsman, M., Jamil, T., Ly, A., Verhagen, J., et al. (2018). Bayesian inference for psychology. Part II: Example applications with JASP. *Psychonomic Bulletin & Review*, *25*, 58–76. https://doi.org/10.3758/s13423-017-1323-7, PubMed: 28685272

Wang, B., van Driel, J., Ort, E., & Theeuwes, J. (2019). Anticipatory distractor suppression elicited by statistical regularities in visual search. *Journal of Cognitive Neuroscience*, *31*, 1535–1548. https://doi.org/10.1162/jocn_a_01433, PubMed: 31180265

Wolfe, J. M. (1994). Guided Search 2.0: A revised model of visual search. *Psychonomic Bulletin & Review*, *1*, 202–238. https://doi.org/10.3758/BF03200774, PubMed: 24203471

Won, B.-Y., & Jiang, Y. V. (2015). Spatial working memory interferes with explicit, but not probabilistic cuing of spatial attention. *Journal of Experimental Psychology: Learning, Memory, and Cognition*, *41*, 787–806. https://doi.org/10.1037/xlm0000040, PubMed: 25401460

Woodman, G. F., & Luck, S. J. (1999). Electrophysiological measurement of rapid shifts of attention during visual search. *Nature*, *400*, 867–869. https://doi.org/10.1038/23698, PubMed: 10476964

Woodman, G. F., & Luck, S. J. (2003). Serial deployment of attention during visual search. *Journal of Experimental Psychology: Human Perception and Performance*, *29*, 121–138. https://doi.org/10.1037/0096-1523.29.1.121, PubMed: 12669752

Worden, M. S., Foxe, J. J., Wang, N., & Simpson, G. V. (2000). Anticipatory biasing of visuospatial attention indexed by retinotopically specific α-band electroencephalography increases over occipital cortex. *Journal of Neuroscience*, *20*, RC63. https://doi.org/10.1523/JNEUROSCI.20-06-j0002.2000, PubMed: 10704517

Zhang, Y., Yang, Y., Wang, B., & Theeuwes, J. (2022). Spatial enhancement due to statistical learning tracks the estimated spatial probability. *Attention, Perception, & Psychophysics*, *84*, 1077–1086. https://doi.org/10.3758/s13414-022-02489-0, PubMed: 35426029

Zhao, G., Liu, Q., Zhang, Y., Jiao, J., Zhang, Q., Sun, H., et al. (2011). The amplitude of N2pc reflects the physical disparity between target item and distracters. *Neuroscience Letters*, *491*, 68–72. https://doi.org/10.1016/j.neulet.2010.12.066, PubMed: 21215298

Zinchenko, A., Conci, M., Töllner, T., Müller, H. J., & Geyer, T. (2020). Automatic guidance (and misguidance) of visuospatial attention by acquired scene memory: Evidence from an N1pc polarity reversal. *Psychological Science*, *31*, 1531–1543. https://doi.org/10.1177/0956797620954815, PubMed: 33119432